Two Improvements to Gardner's Method of Measuring the Hydraulic Conductivity of Non-saturated Media: Accounting for Impedance Effects and Non-constant Imposed Suction Increment

Filip Stanić, Pierre Delage, Yu-Jun Cui, Emmanuel de Laure, Pierre-Antoine Versini, Daniel Schertzer, Ioulia Tchiguirinskaia

Two improvements to Gardner's method of measuring the hydraulic conductivity of non-saturated media: accounting for impedance effects and non-constant imposed suction increment

Filip STANIĆ[1,2], Pierre DELAGE[1], Yu-Jun CUI[1], Emmanuel DE LAURE[1], Pierre-Antoine VERSINI[2], Daniel SCHERTZER[2], Ioulia TCHIGUIRINSKAIA[2]

[1] Ecole des Ponts ParisTech, Navier/CERMES, Marne la Vallée, France

[2] Ecole des Ponts ParisTech, HM&Co, Marne la Vallée, France

Corresponding author:
Filip Stanic
Ecole des Ponts ParisTech
6-8 av. Blaise Pascal, Cité Descartes, Champs-sur-Marne
77455 Marne-la-Vallée cedex 2
France

Email: filip.stanic@enpc.fr
Orcid: 0000-0003-0271-5993

Abstract:

Gardner (1956)'s transient method of measuring the hydraulic conductivity function of unsaturated media has been largely used, together with the improved graphical method proposed by Kunze and Kirkham (1962) to account for the impedance effect resulting from using a low permeability ceramic disk in porous plate testing. These methods are nowadays seldom used, since they have been replaced by numerical back analysis approaches and parameter optimisation algorithms methods. Based on tests carried out on a specific device allowing to determine the water retention and transport properties of water in a coarse granular media at low suctions (up to 50 kPa), it was found necessary to account i) for impedance effects and ii) for the effects of non-constant suction increments, as is often the case when using the hanging column technique. A new method is proposed to account for impedance effects, based on an analytical solution of the equations governing water transfers. The validity of this method is tested by considering experimental data from three distinct materials: a coarse green roof volcanic substrate, poorly graded sand and undisturbed silty clay. Compared to the graphical method Kunze and Kikham's method, it is less operator dependent and hence more objective. It is also simpler than numerical analysis methods, since it does not require any use of numerical code or parameter optimisation algorithm, providing a more direct and reliable access to the investigated parameter. An analytical solution is also proposed to solve the problem resulting from the application of a non-constant suction increment.

Key words: hydraulic conductivity; Gardner's method; impedance effect; non-constant suction increment; Kunze & Kirkham; green roof

Introduction

Gardner's method (Gardner, 1956) was the first analytical method of calculating the hydraulic conductivity of unsaturated porous media by measuring, in the pressure plate apparatus, the transient outflow resulting from an increase in suction, applied to the unsaturated specimen through an increase in air pressure. This method is based on various assumptions, including the linearity of the water retention curve (WRC) and a constant value of the diffusivity D over the suction increment applied (both hypotheses are better fulfilled with small suction increments). Gardner's method doesn't account for the impedance effects of the plate (made up of a high air entry value saturated ceramic porous disk) that may have a significantly lower permeability than that of the saturated specimen. This impedance effect was considered for first time by Miller and Elrick (1958), who proposed an analytical method to account for the flow resistance exerted by the disk, provided the disk permeability was known and the contact specimen/disk was perfect. Rijtema (1959) improved the method by developing a solution based on the permeability ratio between the soil and the disk, valid regardless of the quality of the specimen/disk contact. Finally, Kunze and Kirkham (1962) developed a graphical method based on Miller and Elrick's method, in which particular attention was focused on the accurate determination of initial outflow values, believed to be particularly important with respect to impedance effects. However, this method, based on fitting experimental data against normalized charts to obtain some parameters required to calculate the HCF, obviously presents some degree of subjectivity and operator dependency. More recently, Valiantzas (1990) proposed an analytical method that was not based on the assumption of constant diffusivity. The method was applied on single-step outflow measurements (Doering, 1965) by using an iterative algorithm to determine the relationship between the diffusivity and the water content. The main disadvantage of this method

is that the water retention curve, necessary to make the calculations, has to be determined independently of the hydraulic conductivity function (HCF).

In the past decades, numerical back analysis methods have been preferred to determine the HCF of unsaturated soils, through the simulation of water flow in unsaturated media by numerically solving Richard's equation (Richards, 1931). They account for impedance effects by simulating transient water outflows from two-layered specimens (soil specimen and ceramic disk) submitted to suction increments (Eching and Hopmans, 1993; Eching et al., 1994; van Dam et al., 1994; Durner and Iden, 2011; Schelle et al., 2011; Nasta et al., 2011; Wayllace and Lu, 2011). In these calculations, some pedotransfer functions (Pachepsky and van Genuchten, 2011) are used to describe the hydraulic properties of the soils. By using different optimization algorithms minimizing the deviation between measured and simulated outflows (Duan et al., 1992; Šimunek et al., 2008), an optimal set of parameters of the pedotransfer functions used was obtained. Since the WRC of the investigated materials cannot be always reliably interpreted with pedotransfer functions that depend either on one (Brooks & Corey, 1964) or several semi-empirical parameters (van Genuchten, 1980; Fredlund & Xing, 1994; etc.), the HCF derived through Mualem's approach (1976) does not necessarily provide realistic results (e.g. Khaleel and Relyea, 1995). Moreover, Mualem's model depends on a parameter that accounts for the influences of the pore interconnectivity and of the tortuosity of the medium (Yates et al., 1992; Schaap and Leij, 2000; Peters et al., 2011), a parameter difficult to determine and often excluded from optimization processes. Also, the well-known problem occurring when many parameters are involved in an optimization algorithm is that the solution is not unique, with various convenient parameter combinations.

Given the advantages and drawbacks of existing methods, a new and simple analytical approach to account for impedance effects in the determination of the HCF of unsaturated soils is proposed in this paper, together with an approach to account for non-constant imposed suction increment. The validation of the method is carried out based on experimental data from three different materials, i.e. a coarse material used as substrate in an urban green roof located in the Paris area and called the "Green Wave" because of its wavy shape (Versini et al. 2018, Stanic et al. 2019), a poorly graded sand and an undisturbed silty clay (Wayllace and Lu 2011). This analytical method is simpler than numerical back analysis methods since it does not require the use of any numerical code and optimization process. It is also not affected either by any subjective graphical method like in the traditional Kunze and Kirkham's method.

Experimental investigations

This work was initially developed when investigating the water retention and transfer properties of a volcanic coarse substrate used in an urban green roof in the Paris area, detailed in Stanic et al. (2019). The device, material and data of this work will be recalled and considered in more details. The validity of the method will then be further established by also considering the experimental data obtained on two quite different materials (a poorly graded sand and an undisturbed silty clay) published by Wayllace and Lu (2011).

Stanic et al. (2019)'s data

The device developed by Stanic et al. (2019), presented in Figure 1, consists of a metal cell (inner diameter 7×10^{-2} m, height 5×10^{-2} m, cross sectional area $A = 3.848 \times 10^{-3}$ m^2) in which a 2.4×10^{-2} m height specimen is placed on a high air entry value (HAEV) ceramic porous disk of thickness $\Delta z_d = 5 \times 10^{-3}$ m. The air entry value of the disk is 50 kPa and its saturated

permeability K_d = 4.02 x 10^{-8} m/s. The porous disk is connected to a thin flexible tube (5 x 10^{-3} m inner diameter) connected, through a valve V1, to a mobile device aimed at accurately imposing, at the other extremity of the flexible tube, a water level lower than that of the specimen top. This hanging column device allows, through the HAEV ceramic porous disk, to apply a suction measured by the difference in height (h_k) between the controlled lower level (left), and that of the specimen top (right). The maximum height allowed by the system is equal to 5 m, corresponding to a maximum suction of 50 kPa. Figure 1 shows the two options permitted by the device. In the case of large water exchanges with the specimen, like those occurring close to full saturation, the configuration described in a), in which a constant level is imposed in the inner tube by an overflow system, is used. The larger excess of water extracted is collected in an outer tube of larger inner diameter (1.5 x 10^{-2} m). When less water is extracted, a more accurate monitoring - described in b) - is allowed by following the change in level of the extracted water in the inner tube (5 x 10^{-3} m inner diameter, 8 x 10^{-3} m outer diameter). In this case, lowering the mobile device to a fixed position results in applying a non-constant suction at the specimen, since the water extracted progressively refills the inner tube.

The Figure also shows that the thin tube is connected, through valve V2, to a high precision (0.1 mm) differential pressure transducer, that gives the difference in pressure between the thin tube and a reference constant water height, previously adjusted at optimum level. In the configuration at constant imposed suction, valve V3 is opened and V2 closed, and the pressure transducer measures the change in hydrostatic pressure resulting from the increase in water level in the outer tube. Alternatively, when valve V3 is closed and V2 open, the transducer measures the pressure corresponding to the changing height in the inner tube.

The material investigated is the volcanic substrate used for covering the "Green Wave" in the city of Champs-sur-Marne in France (Versini et al., 2018). From a hydrological point of view, the water retention and transfer properties of this substrate are necessary to investigate the mitigation and delay of the runoff peak on the green roof (Stovin et al., 2015), especially in the near saturated zone (Vogel et al., 2001). The substrate used is a coarse granular material with 4 % of organic matter, an average grain density of 2.35 Mg/m^3 and a density of 1.4 Mg/m^3, with D_{50} = 1.5 mm, 15% particles smaller than 80 µm and a curvature coefficient ($D_{30}^2/(D_{10}\ D_{60})$) of 1.95. The saturated hydraulic conductivity of the substrate is K_s = 8.11 x 10^{-6} m/s, and its water retention curve is given in Figure 2 (Stanic et al., 2019).

Wayllace and Lu (2011)'s data

Wayllace and Lu (2011) developed a transient water release and imbibition (TWRI) method for determining the WRC and HCF of two materials along the drying and wetting paths, by imposing, through the axis translation method, two suction increments for draining water from the soil specimen, followed by a suction decrease allowing subsequent water imbibition. The TWRI apparatus consisted of i) a flowcell accommodating a soil specimen of 6.07 cm diameter placed on 300 kPa HAEV ceramic disk (saturated permeability K_d = 2.5x10^{-9} m/s, thickness Δz_d = 3.2 x 10^{-3} m, area A = 2.894 x 10^{-3} m^2), ii) a pressure regulator connected to cell top and iii) a water jar placed on a weight scale connected to cell bottom to collect the drained outflow (more details in Wayllace and Lu, 2011).

During drainage, a first imposed suction increment was fixed (3 kPa for sand and 5 kPa for silty clay), just above the specimen air entry values, small enough to just initiate the outflow from the specimen, while the second step was significantly larger (about 300 kPa).

Wayllace and Lu investigated two different soils: a remoulded poorly graded sand compacted to a porosity of 0.39 and an undisturbed silty clay with a porosity 0.44. The values of the saturated hydraulic conductivities of these soils are K_s = 2.1 x 10^{-6} m/s and 1.1 x 10^{-7} m/s, respectively. The significantly lower saturated permeability of the ceramic disk clearly indicates that impedance effects have to be accounted for when analysing the outflow data.

Analytical methods of determining the hydraulic conductivity of unsaturated materials

The two most used analytical methods of determining the hydraulic conductivity of unsaturated materials are Gardner's method (with no impedance effect) and Kunze and Kirkham's method, in which impedance effects are accounted for. The assumptions made in Gardner's method (linearity of the water retention curve and constant diffusivity along the small suction step applied) allow to transform Richard's equation (Richards, 1931) into an equation similar to Fourier's heat equation, comparable to the Terzaghi-Fröhlich equation (Terzaghi & Fröhlich, 1936) that governs the consolidation of saturated soils. The analytical solution using Fourier's series can then be used. When using Stanic et al. (2019)'s device, it was preferred to express suction and water pressures in terms of water height $h_k\,(z,\,t)$ [L], as the sum of the initial suction $h_k\,(z,\,0)$ and the time depending change of suction $\Delta h_k\,(z,\,t)$. Given that the imposed suction increment Δh_i (index i for "imposed") is immediately transferred to the bottom of the specimen ($\Delta h_k\,(z=0,\,t) = \Delta h_i = const.$), the ratio $\Delta h_k\,(z,\,t) \,/\, \Delta h_i$ is analog to the degree of consolidation in Terzaghi-Fröhlich's theory, expressed using Fourier's series as follows:

$$\Delta h_k(z,t) = \Delta h_i \left(1 - \frac{4}{\pi}\sum_{n=1,3,5\ldots}^{\infty} \frac{1}{n} e^{-(n\pi/2)^2\, t\mathrm{D}(h_k)/H_s^2} \sin\frac{n\pi z}{2H_s}\right) \quad (1)$$

183 in which H_s is the specimen thickness [L], and $D(h_k) = K(h_k)/C(h_k)$ is the (constant) diffusivity
184 value [L^2/T] at suction h_k, which is equal to the ratio between the hydraulic conductivity value
185 $K(h_k)$ [L/T] and the slope of the water retention curve along the applied suction step $C(h_k)$ [L^{-1}].
186 Since the first derivative at the specimen bottom $\frac{\partial h_k(z,t)}{\partial x}\Big|_{z=0} = \frac{\partial \Delta h_k(z,t)}{\partial x}\Big|_{z=0}$ governs the drained
187 outflow, assuming a linear water retention curve and integrating the flux in time, the total water
188 content at time t can be obtained. The changes in water volume are finally expressed as:

189 $$V(t) = V_\infty \left(1 - \frac{8}{\pi^2}\sum_{n=1,3,5\ldots}^{\infty} \frac{1}{n^2} e^{-(n\pi/2)^2\, t\, D(h_k)/H_s^2}\right) \quad (2)$$

190 in which V_∞ is the total volume [L^3] of the outflow drained from the soil specimen after imposing
191 Δh_i. The total extracted volume is given by: $V_\infty = \frac{H_s \Delta h_i K(h_k) A}{D(h_k)} = H_s \Delta\theta A$ ($\Delta\theta$ is the change of the
192 water content [-] and A is the cross-sectional area of the specimen [L^2]).
193 Without considering the outflow at very small t, Gardner provided a convenient relation by
194 keeping only the first term of Fourier series:

195 $$\ln(V_\infty - V(t)) = ln\left(\frac{8V_\infty}{\pi^2}\right) - \left(\frac{\pi}{2H_s}\right)^2 D(h_k)t \quad (3)$$

196 Indeed, Gardner's experimental data showed that the changes in the first term with respect to
197 time become linear after some time period (see Stanic et al., 2019), providing a reliable
198 estimation of the diffusivity $D(h_k)$ from the slope of the ln (V_∞ - V) curve. The estimation is more
199 accurate with small imposed suction increments, since $D(h_k)$ is the average diffusivity value
200 along it. The hydraulic conductivity $K(h_k)$ at suction h_k is derived by using the water retention
201 properties parameter $C(h_k)$.
202 When the hydraulic conductivity of the HAEV disk is significantly smaller than that of the
203 specimen, the suction increment Δh_i imposed at the bottom of the porous disk is not immediately
204 transferred to the specimen due to impedance effects. To cope with this issue, Kunze and

Kirkham (1962) proposed a graphical method based on the solution of Miller and Elrick (1958). The solution is graphically presented through various curves showing the changes in $V(t)/V_\infty$ with respect to the variable $\lambda_1^2 D(h_k)t/H_s^2$, in which parameter λ_1 is the first solution of the equation $a\lambda_n = cot(\lambda_n)$ (a is the ratio between the impedance of the ceramic disk and that of the sample). The various curves correspond to various values of parameter a. By shifting the chosen theoretical curve along the $\lambda_1^2 D(h_k)t/H_s^2$ axis, the best agreement with experimental data (presented in the form $V(t) / V_\infty$ versus t) is obtained and a reference time t_{RP} is graphically determined for $\lambda_1^2 Dt / H_{soil}^2 = 1$. Kunze and Kirkham (1962) remarked that only a portion of the experimental data corresponded to the theoretical curves, so they recommended to rather fit the curves at small times, for which more accurate values of λ_1^2 are obtained. Finally, the diffusion coefficient is calculated as $D(h_k) = H_s^2 / \lambda_1^2 t_{RP}$ and the hydraulic conductivity as $K(h_k) = D(h_k) \Delta\theta/\Delta h_k$.

As commented in the Introduction, this graphical method is nowadays rarely used and has been replaced by numerical back analysis of water outflow under imposed suction increments.

A new method to account for impedance effects

Due to the impedance effects resulting from the low permeability of the HAEV ceramic porous disk, the suction increment Δh_i applied at the disk bottom at $t = 0$ is not instantaneously transmitted at the top, where the initial suction is equal to the specimen suction h_k. As an alternative to existing methods of accounting for impedance effects, it is proposed to first apply Darcy's law to the saturated porous disk of thickness Δz_d, saturated permeability K_d and cross sectional area A, similarly as in Eching et al. (1994). One obtains the following expression of the drained outflow $Q(t)$ [L^3/T]:

$$Q(t) = -K_d \frac{\Delta h_k(z=0,t) - \Delta h_i}{\Delta z_d} A = \frac{\Delta V(t)}{\Delta t} \quad (4)$$

where ΔV [L^3] is the extracted water volume during the time interval Δt. The following relation gives the changes in the increment of suction at the specimen's bottom:

$$\Delta h_k(z = 0, t) = \Delta h_i - \Delta z_d \frac{Q(t)}{AK_d} \quad (5)$$

This relation indicates that the change with respect to time of the suction applied at the specimen bottom can be derived from the monitoring of the drained outflow $Q(t)$, that depends on both the permeability of the porous disk and the combined effects of the water retention and transfer properties of the unsaturated specimen. Theoretically, the case with no impedance effect in which $\Delta h_k\ (z = 0,\ t) = \Delta h_i$ is met with porous disks of large permeability, when $K_d >> Q(t)/A$.

Based on the time superposition principle (Hantush, 1964; Stanic et al., 2017 among others), it is hence proposed i) to decompose a suction increment at the specimen bottom $\Delta h_k\ (z = 0,\ t)$ as the sum of a number N_s of very small successive suction increments $\Delta h_m = \Delta h_i/N_s$, occurring at time t_m, ii) to apply the analytical solution (Eq. 1) to each suction increment and iii) to superpose in time all suction increments, giving the following expression of the suction changes:

$$\Delta h_k(z,t) = \sum_{m=1}^{N_s} \Delta h_m \left(1 - \frac{4}{\pi} \sum_{n=1,3,5\ldots}^{\infty} \frac{1}{n} e^{-(n\pi/2)^2 (t-t_m) \mathrm{D}(h_k)/H_s^2} \sin \frac{n\pi z}{2H_s}\right) \quad (6)$$

resulting in the following expression of extracted volume, once integrated in z along the sample height:

$$\mathrm{V}(t) = \frac{V_\infty}{N_s} \sum_{m=1}^{N_s} \left(1 - \frac{8}{\pi^2} \sum_{n=1,3,5\ldots}^{\infty} \frac{1}{n^2} e^{-(n\pi/2)^2 (t-t_m) \mathrm{D}(h_k)/H_s^2}\right) \quad (7)$$

An application of this approach by using the device of *Figure 1* on the coarse substrate (Stanic et al. 2019) is given in *Figure 3*, in which the monitored changes in volume with respect to time during the application of a first suction step (Δh_i = 0.185 m) from the initial zero suction state are

presented. This suction increment resulted in a decrease in water content $\Delta\theta = 0.16$ from an initial value at zero suction of 0.395.

Figure 3a indeed shows that, due to impedance effects, a delay of around 5 hours is needed before suction at the specimen bottom $\Delta h_k\ (z = 0,\ t)$ reaches the imposed suction increment Δh_i. Assuming only a single suction step ($N_s = 1$), $\Delta h_{m=1}$ is equal to Δh_i, thus Equation (7) becomes identical to Gardner's method (Equation 2) – see *Figure 3b*. On the other hand, *Figure 3c* illustrates the influence of non-single successive suction steps ($N_s = 3$, $\Delta h_m = \Delta h_i / 3$), where time t_m are equal to the t values for which Equation (5) is identical to the sum of all previous successive suction steps: $\Delta h_k(z = 0, t) = \sum_1^{m-1} \Delta h_m$ (*Figure 3d*). After determining t_m, the calculation of $V(t)$ (Equation 7) can be made by using MATLAB. The correct value of diffusivity is obtained the same way as with the standard Gardner's method, by fitting the theoretical results with the experimental ones. From *Figure 3d*, it is obvious that, for the same diffusivity value $D(h_k)$, Gardner's method significantly overestimates the measured $V(t)$ value, compared to the method proposed in this study. However, it can be noticed that Equation (7) shows multiple discontinuities at $t = t_m$ that are due to the additional suction steps adopted at those times. For that reason, it is necessary to decompose $\Delta h_k\ (z=0,\ t)$ in very small suction steps that can secure a reasonably continuous $V(t)$ function. Since the calculation method is not time consuming, it is proposed to adopt $N_s = 1000$, a number large enough to satisfy continuity of $V(t)$ function for various materials.

Figure 4 presents a simplified scheme of the implementation of step 1 (constant imposed suction increase), together with the experimental and calculated suction and volume changes with, and without, impedance effects. In the top left graph are presented the changes in suction along the sample's height at different times. Without any impedance effects (dotted lines), the boundary

suction condition at bottom is fixed and equal to Δh_i, and suction profiles are comparable to typical excess pore pressure dissipation curves, as described in Terzaghi-Frölich's theory (Equation 1) of consolidation of saturated soils (calculated with a fitted value $D(h_k) = 0.75 \times 10^{-7}$ m^2/s). In the case of impedance effects, the suction profiles (solid lines) are calculated using Equation (6) with $N_s = 1000$, after fitting parameter $D(h_k)$ to a value of 1.2×10^{-6} m^2/s. The calculated changes in suction with time at specimen bottom show how the boundary conditions progressively reach the Δh_i condition imposed at $t = 0$ at the bottom of the porous disk.

In the top right graph are presented the suction changes at specimen bottom (Δh_k ($z = 0$, t)) with respect to a logarithmic scale of time, to better observe the changes at small times when impedance effects are the most significant. Connected black dots present Δh_k (z=0, t), calculated using measured volumes and Darcy's law (Equation 5), that gradually reaches Δh_i (dashed line) imposed at the disk bottom. For decomposing calculated Δh_k $(z=0, t)$ curve, $N_s = 1000$ successive suction steps are used. It can be noticed that ratio values Δh_k $(z=0, t)$ / Δh_i (x axis) for $z = 0$ at different times (t_1 to t_4) correspond to ones in the middle graph (y axis) for the same t.

Finally, the bottom right graph presents a comparison of the calculated values of $V(t)/V_\infty$ (in a time logarithmic scale) using Gardner's method, Kunze and Kirkham's method and that developed in this work (Kunze and Kirkham's non-dimensional time variable $\lambda_1^2 D(h_k) t_{RP} / H_s^2$ is also reported on the top x-axis of the graph). Fitting our experimental data following Kunze and Kirkham's method provided $\lambda_1 = 0.097$ and $t_{RP} = 2750$ s, with $a = 10$ (a is ratio between the disk and the specimen permeability). If one follows the recommendation of the authors to fit only a portion of measurements at small times with theoretical curves, the results could change significantly. In case of step 1, the theoretical curves with much smaller parameter a ($a = 0.2$ or 0.142) provide the best agreement with measured volumes at small times, which leads to lower

values of $K(h_k)$. However, overall agreement is less satisfactory than for the adopted case with a = 10. On the contrary, adopted theoretical curve a = 10 and curve a = 1000 are rather similar, thus it is difficult to distinguish the difference between both. Since a = 1000 provides two orders of magnitude higher value of hydraulic conductivity (even higher than the saturated hydraulic conductivity) than a = 10, a value of a = 10 is finally adopted. The Figure shows excellent agreement between experimental data and both Kunze and Kirkham and the proposed method. Unsurprisingly, the extracted volume estimated by Gardner's method for times smaller than 1 *h* is higher than the measured one and that calculated with two other methods.

Given that the calculation of the Fourier series of Equations (1), (2), (6) and (7) may be found somewhat tedious, one tested the approximated empirical formula proposed by Sivaram and Swamee (1977) in their simplified approach to solve Terzaghi - Fröhlich's consolidation equation, as follows:

$$\frac{V(t)}{V_\infty} = \left(\frac{4tD(h_k)}{\pi H_s^2}\right)^{0.5} \left(1 + \left(\frac{4tD(h_k)}{\pi H_s^2}\right)^{2.8}\right)^{-0.179} \quad (8)$$

Equation (8) can be substituted in all equations where Fourier series appear, changing Equation (7) to the following:

$$V(t) = \frac{V_\infty}{\Delta h_i}\left[\sum_{m=0}^{N_s} \Delta h_m - \sum_{m=0}^{N_s} \Delta h_m \left(1 - \left(\frac{4(t-t_m)D(h_k)}{\pi H_s^2}\right)^{0.5} \left(1 + \left(\frac{4(t-t_m)D(h_k)}{\pi H_s^2}\right)^{2.8}\right)^{-0.179}\right)\right] \quad (9)$$

The corresponding curve, also plotted in *Figure 4*, shows excellent comparability between this expression (9) and the calculation of Equation (7). For sake of simplicity, it is hence proposed to adopt expression (9).

A new method to account for non-constant imposed suction increment

As described in *Figure 5*, the overflow system used in Stanic et al. (2019) (*Figure 1a*), that imposes a constant suction, is used to measure larger water extracted volume thanks to the larger diameter of the outer tube, whereas good precision is achieved for smaller extracted volumes by using the smaller diameter inner tube. In such conditions, the suction increment imposed at $t = 0$ by moving the mobile device downwards is affected by a subsequent progressive increase in water level in the tube when water is extracted from the specimen. In the test program carried out on the volcanic substrate (see Stanic et al. 2019), large extracted volumes of water were observed during the two first suction steps applied from the zero-suction initial state (Δh_i = 0.185 and 0.212 m, respectively). Starting from step 3 (initial suction 0.397 m and Δh_i = 0.128 m), it was observed that *i*) extracted water volumes were too small to be measured by the outflow system and *ii*) the unsaturated hydraulic conductivity of the unsaturated substrate was one order of magnitude smaller than that of the ceramic porous disk (K_d = 4.02 x 10^{-8} m/s). In this context, it was necessary to examine how to determine the hydraulic conductivity with a non-constant suction imposed condition.

The progressive increase in water level causes a gradual decrease in suction $\Delta h_k\ (z=0,\ t)$ imposed at the specimen bottom. Since the increase in water level is caused by the outflow drained from the specimen, the water balance equation can be written in the following way:

$$-\frac{d\Delta h_k(z=0,t)}{dt} a_{it} = Q(t) = \frac{dV(t)}{dt} \quad (10)$$

where a_{it} is the cross-section area [L^2] of the small inner tube in which outflow is collected. Since there is no impedance effect, $V(t)$ can be substituted with Gardner's solution (Equation 2),

by substituting V_∞ by $\frac{H_s \Delta h_k(z=0,t) K(h_k) A}{\mathrm{D}(h_k)}$, thus replacing the constant Δh_i by the non-constant $\Delta h_k(z=0, t)$. The outflow $Q(t)$ then becomes equal to:

$$Q(t) = \frac{dV(t)}{dt} = \frac{d\Delta h_k(z=0,t)}{dt} \frac{H_s K(h_k) A}{D(h_k)} F(t) + \frac{H_s \Delta h_k(z=0,t) K(h_k) A}{D(h_k)} F'(t) \quad (11)$$

where $F(t) = 1 - \frac{8}{\pi^2} \sum_{n=1,3,5\ldots}^{\infty} \frac{1}{n^2} e^{-(n\pi/2)^2 \, \mathrm{t} \, \mathrm{D}(h_k)/H_s^2}$ and $F'(t) = \frac{dF}{dt}$.

After introducing Equation (11) into Equation (10), the variables can be separated, leading to:

$$-\int_{\Delta h_i}^{\Delta h_k(z=0,t)} \frac{d\Delta h_k(z=0,t)}{\Delta h_k(z=0,t)} = \int_0^t \frac{F\prime(t) \frac{H_s K(h_k) A}{D(h_k)}}{a_{it} + F(t) \frac{H_s K(h_k) A}{D(h_k)}} dt \quad (12)$$

After integrating both sides of Equation (12), the following obtains:

$$\ln\left(\frac{\Delta h_i}{\Delta h_k(z=0,t)}\right) = \ln\left(1 + F(t) \frac{H_s K(h_k) A}{a_{it} D(h_k)}\right) \quad (13)$$

The expression of $\Delta h_k(z=0, t)$ is then derived as follows:

$$\Delta h_k(z=0,t) = \frac{\Delta h_i}{1 + F(t) \frac{H_s K(h_k) A}{a_{it} D(h_k)}} \quad (14)$$

By knowing that $V(t) = a_{it}\left(\Delta h_i - \Delta h_k(z=0,t)\right)$, and $V(t_\infty) = V_\infty$, the following equation can be written:

$$V_\infty = a_{it}\left(\Delta h_i - \Delta h_k(z=0,t_\infty)\right) = \frac{H_s \Delta h_k(z=0,t_\infty) K(h_k) A}{\mathrm{D}(h_k)} \quad (15)$$

$$\frac{H_s K(h_k) A}{a_{it} \mathrm{D}(h_k)} = \frac{\Delta h_i}{\Delta h_k(z=0,t_\infty)} - 1 \quad (16)$$

After introducing the last expression into Equation (14), the final forms of $\Delta h_k(z=0, t)$ and $V(t)$ are obtained:

$$\Delta h_k(z=0,t) = \frac{\Delta h_i}{1 + F(t)\left(\frac{\Delta h_i}{\Delta h_k(z=0,t_\infty)} - 1\right)} \quad (17)$$

$$V(t) = a_{it}\Delta h_i\left(1 - \frac{1}{1+F(t)\left(\frac{\Delta h_i}{\Delta h_k(z=0,t_\infty)}-1\right)}\right) \quad (18)$$

For t = 0, $F(t)$ = 0, so $\Delta h_k(z=0,\ t=0) = \Delta h_i$ and $V(t)$ = 0. On the contrary, for $t = t_\infty$, $F(t)$=1, leading to $\Delta h_k(z=0,\ t=t_\infty)$ and $V(t) = a_{it}\left(\Delta h_i - \Delta h_k(z=0, t_\infty)\right) = V_\infty$. Please note that Fourier series $F(t)$ is identical as in Equation (2), thus it can be substituted using the empirical expression (8), as previously explained, and introduced into Equation (18) for sake of simplicity.

To calculate suction profiles, the non-constant boundary condition (Equation 17) is decomposed as in the case of the impedance effect, and Equation (6) is applied afterwards. *Figure 5* illustrates a simplified scheme of the implementation of steps 4 (a) and 11 (b) (non-constant imposed suction), together with the measured and calculated suction and volume changes when considering constant and non-constant imposed suction increments. It is indicated in the Figure that the initial suctions for steps 4 and 11 are 0.489 m and 3.227 m, respectively, while the imposed suction increments are 0.321 m and 0.822 m, with 17 % and 5 % of suction step change during the test, respectively. The top graphs present the calculated suction profiles at different times for 2 cases: i) constant suction step $\Delta h_i = \Delta h_k(z=0, t_\infty)$ described using Equation (1) and ii) non-constant suction increment $\Delta h_i = \Delta h_k(z=0, t)$ described with Equation (6). In step 4 (*Figure 5*a) the boundary condition $\Delta h_k(z=0, t)$ changes between Δh_i at t = 0 and $\Delta h_k(z=0, t_\infty) = 0.83\Delta h_i$ at t_∞ (solid lines), while it remains fixed at value $0.83\Delta h_i$ in the case of constant suction step. Note that suction change is less significant in step 11 (5 %) and suction profiles for two different boundary conditions are rather similar (see *Figure 5b*).

In the middle graph of *Figure 5*a, calculated changes in $\Delta h_k(z=0, t)$ (Equation 17 - solid line) are compared with measured changes in water level, while calculated (Equation 18) and measured drained volumes are compared in the bottom graph. The difference between the non-constant

($\Delta h_k(z=0,\ t)$) and constant ($\Delta h_k(z=0,\ t_\infty)$) suction increment is more significant at initial time, right after imposing Δh_i, while the largest difference in drained volumes between our method and Gardner's method is observed after t_2 = 25 min. Method proposed in this work shows the best agreement for $D(h_k)$ = 4.3x10^{-8} m^2/s (the same value is adopted for Gardner's method), while Kunze & Kirkham's theoretical curve with parameters a = 0, t_{RP} = 4400 s and λ_1^2 = 2.467 also shows satisfying agreement at small times.

All three methods show almost identical agreement with measured volumes when the overall suction step change is negligible, like in step 11 (bottom graph in *Figure 5b*). Moreover, the top graph in *Figure 5b* shows rather similar suction profiles for the cases with constant and non-constant suction increments.

Determination of hydraulic conductivity values

Green Wave substrate (Stanic et al., 2019)

By analyzing the evolution of drained outflow for different suction steps, the change of hydraulic conductivity with respect to increased suction is obtained. *Figure 6* shows the changes in hydraulic conductivity obtained by using the three different approaches: Gardner's method (triangles), Kunze & Kirkham's method (squares) and the methods proposed in this work (circles). Hydraulic conductivity values are presented in logarithmic scale. All 3 methods are applied on steps 1, 2, 3, 4, 8, 11 and 12, for which stable and reliable volume change measurements are obtained at small times. Note that we also present in the Figure the hydraulic conductivity values for steps 5, 6, 7, 9 10 and 13, that were obtained by using standard Gardner's method, based on volume change measurements at larger times (Equation 3).

395 Steps 1 and 2 were constant suction steps (with the overflow system of *Figure 1a*) whereas the
396 remaining steps correspond to non-constant suction increments (see *Figure 1b*). The saturated
397 hydraulic conductivities of both the specimen (K_s) and the ceramic disk (K_d) were determined
398 using a constant head permeability test described in details in Stanic et al. (2019).
399 *Figure 6* shows that both our method and Kunze & Kirkham's one provide very similar results
400 for the first two steps where significant impedance effect occurs. In this range, Gardner's method
401 unsurprisingly provides significantly lower $K(h_k)$ values because it integrates the effect of the
402 low hydraulic conductivity of the disk. In case of steps 8, 11 and 12, where the imposed suction
403 step changes less than 5 % where no impedance effect occurs, all methods provide comparable
404 results.
405 From a hydrological point of view with respect to the functioning of the Green Wave made up of
406 the volcanic material investigated here, the values of $K(h_k)$ in the low suction regime present the
407 greatest interest, since they have the most significant influence on the hydrological responses of
408 the substrate. As shown in *Figure 6*, this zone (first 4 steps) is precisely that in which the most
409 significant differences are observed between the methods used, showing the advantage of our
410 method, that is less operator dependent compare to that of Kunze and Kirkham.

411 **Poorly graded sand and silty clay (Wayllace and Lu, 2011)**

412 Among the transient outflow data from Wayllace and Lu (2011), only the first and smaller of the
413 two applied suction steps was considered on both specimens because i) our method assumes
414 constant diffusivity, a hypothesis only acceptable for small suction increments and ii) the
415 impedance effect is more significant at initial steps, when the permeability of the soil is
416 significantly larger than that of the ceramic disk.

In Figure 7a-top is presented the change of $\Delta h_k(z=0, t)$ for the poorly graded sand specimen (H_s = 2.67 x 10^{-2} m) resulting from imposing Δh_i = 0.3 m. Figure 7a-bottom presents the corresponding change in $V(t)$ (circles) drained from the specimen (V_∞ = 4.66 x 10^{-6} m^3). The method proposed in this work (Equations 7 and 9 – solid and dashed lines), Gardner's (Equation 2 – dotted line) and Kunze and Kirkham's method (dash-dot line) are compared to measured outflows. The same data are presented in Figure 7b for the silty clay specimen (H_s = 2.41 x 10^{-2} m), for which Δh_i = 0.5 m and the total drained volume V_∞ = 1 x 10^{-6} m^3.

The bottom graphs in Figure 7a show that our method and Kunze & Kirkham's method compare quite well whereas Garner's method overestimates the outflow values at small times, like for the Green Wave substrate (Figure 4). On the contrary, in case of the silt clay specimen (Figure 7b-bottom) both Gardner's and Kunze & Kirkham's methods overestimate the outflows at small times, whereas our method shows excellent agreement with measurements along the whole time range. Due to the poor agreement at small times, Kunze & Kirkham's analytical curve was fitted with measurements at larger times (the parameters for this method are indicated in Figure 7 and in Table 1).

Based on the adjusted $D(h_k)$ values in the case of Gardner's and of our method, and parameters a, t_{RP} and λ_1^2 in case of Kunze & Kirkham's method (Table 1), the values of the hydraulic conductivity for the first step were determined. In case of poorly graded sand, the following values were obtained: $K(h_k$ = 0.3 m$)$ = 2.01x10^{-9} m/s (Gardner), 2.81x10^{-9} m/s (our method) and 4.58x10^{-9} m/s (Kunze & Kirkham). For the silty clay: $K(h_k$ = 0.5 m$)$ = 2.29x10^{-9} m/s (Gardner), 4.01x10^{-9} m/s (our method) and 6.37x10^{-9} m/s (Kunze & Kirkham). Based on the data from our method and Kunze & Kirkham's method, it can be concluded that the impedance effect does occur (we have $K(h_k) > K_d$ for both methods and both soils), but it is not significant, since the

obtained $K(h_k)$ values are the same order of magnitude as K_d (~ 10^{-9} m/s). Unsurprisingly, in the case of Gardner's method, $K(h_k)$ is slightly lower than K_d for both soils.

On the occurrence of impedance effects

The occurrence of impedance effects can clearly be observed in Figure 5 during steps 1 to 3, by comparing the data of Gardner's method with the two other ones accounting for impedance effects. Unsurprisingly, the apparent HC derived from Gardner's method is significantly smaller than other estimations at low suctions due to the underestimation resulting from the low permeability ceramic disk. However, this difference decreases quite rapidly, since a convergence of the three methods is observed at a HC of 2 x 10^{-8} m/s, to compare to the twice larger HC value of the ceramic disk (4.02 x 10^{-8} m/s).

The most convenient way to clarify the importance of impedance effects is by analysing the evolution of the ratio $\Delta h_k(z=0,t) / \Delta h_i$, calculated by using Equation (5). The faster the ratio gets close to 1, the less significant impedance effects are, and vice versa. It seems reasonable in this regard to define a criterion based on the relative time t / t_∞ (t_∞ is the time at which equilibrium is reached) at which $\Delta h_k(z=0, t) / \Delta h_i$ gets close enough to 1 (ex. 0.95). Based on experience, we believe that impedance can be ignored if $\Delta h_k(z=0,t) / \Delta h_i$ reaches 0.95 within the first 5 % of the step duration, leading to a criterion $t_c / t_\infty = 0.05$. After dividing both sides of Equation (5) by Δh_i and introducing the proposed criterion, the following is obtained:

$$\frac{V(t_c)}{t_c A} < 0.05 \frac{\Delta h_i}{\Delta z_d} K_d, \qquad t_c = 0.05 t_\infty \tag{19}$$

Equation (19) shows that besides the specimen permeability K_d, the values of imposed suction increment Δh_i and stone thickness Δz_d also affect the impedance. For the data presented in Figure 4 (coarse material), Figure 7a (sand) and Figure 7b (silty clay), the values of the left side of Equation (19) are 1.2 x 10^{-6}, 6.8 x 10^{-8} and 9.6 x 10^{-8} m/s, respectively, while the values on the

463 right side are 1.5 x 10^{-7}, 1.17 x 10^{-8} and 1.95 x 10^{-8} m/s. Equation (19) is hence not satisfied in
464 none of the three cases, meaning that impedance effects cannot be neglected. In case of step 2 of
465 the coarse substrate, the left and right side of Equation (19) are almost identical, which is in
466 agreement with the obtained $K(h_k)$ value that is rather close to K_d (see *Figure 6*).

467 Conclusion

468 As initially shown by Gardner (1956), a convenient way to measure the hydraulic conductivity of
469 unsaturated media can be derived from monitoring the water outflow of an unsaturated specimen
470 submitted to a suction step. The method has been improved by Kunze and Kirkham (1962) to
471 account for the impedance effects due to the low (saturated) hydraulic conductivity of the
472 ceramic disks used in pressure plate devices. However, the graphical method that they proposed
473 at that time is no longer used nowadays, because numerical back analysis of water transfers in
474 unsaturated specimens submitted to suction step proved to be more relevant, accurate and easy to
475 use.
476 In this context, two improvements to Gardner's method were proposed in this paper i) to account
477 for impedance effect in a simpler and more objective way than in Kunze and Kirkham's
478 graphical method and ii) to account for conditions in which non-constant suction increment is
479 applied, as is often the case in hanging column techniques (e.g. Stanic et al. 2019).
480 The experimental data from various kinds of materials analysed (coarse substrate, poorly graded
481 sand and undisturbed silty clay) in this work showed that the proposed simple analytical method
482 fairly well accounts for the impedance effects of the ceramic disk. This method is considered as
483 more reliable than Kunze & Kirkham's graphical method, especially in the case of significant
484 impedance effect, because it is not dependent of the difficulty in choosing the best fitting

theoretical curve, among the family of curves provided by Kunze & Kirkham. The proposed method, based on the analytical resolution of the water transfer equations in the different parts of the system, only requires the accurate monitoring of outflow measurements, a requirement that is typical for any method for determining the hydraulic conductivity of multiphase porous material. The boundary condition in which a non-constant suction increment is applied, which is often the case when using the hanging column technique, was also treated analytically to be applied in the (larger) suction area in which no impedance effect has to be considered, with also good agreement between measured and calculated values. It has also been shown, that the simplified equation of Sivaram and Swamee (1977) could successfully replace the analytical solution in Fourier series, which simplifies the use and improves the efficiency of the method. Compared to numerical back analyses method, this method is considered simpler in the sense that it does not require the use of any numerical simulations and back analysis with optimization algorithms to determine the relevant parameters, since the analysis of outflow data and the derivation of hydraulic conductivity value is much more straightforward.

Acknowledgments:

The authors greatly acknowledge the Inter-laboratory PhD Merit Scholarship, provided by Ecole des Ponts ParisTech to the first author, which made this collaborative work possible. A partial financial support by the Chair “Hydrology for resilient city” endowed by Veolia is also highly acknowledged. Authors provided supporting information.

References:

Brooks, R.H., A. T. Corey. (1964). Hydraulic properties of porous media. *Hydrology papers,* no. 3, Colorado State University, Fort Collins.

Doering, E. J. (1965). Soil-water diffusivity by the one-step method. *Soil Science*, 99, 322-326.

Duan, Q., Sorooshian, S., Gupta, V. (1992). Effective and Efficient Global Optimization for Conceptual Rainfall-Runoff Models. *Water Resour. Res.,* 28(4), 1015-1031. DOI:10.1029/91WR02985.

Durner, W., and Iden, S. C. (2011). Extended multistep outflow method for the accurate determination of soil hydraulic properties near water saturation. *Water Resour. Res.*, 47, DOI:10.1029/2011WR010632.

Eching, S. O. and Hopmans J. W. (1993). Optimization of Hydraulic Functions from Transient Outflow and Soil Water Pressure Data. *Soil Sci. Soc. Am. J.*, 57, 1167-1175.

Eching, S. O., Hopmans J. W., & Wendroth O. (1994). Unsaturated Hydraulic Conductivity from Transient Multistep Outflow and Soil Water Pressure Data. *Soil Sci. Soc. Am. J.*, 58, 687-695.

Fredlund, D. G. and Xing, A. (1994). Equations for the soil characteristic curve. *Can. Geotech. J.,* 31, 521-532.

Gardner, W. R. (1956). Calculation of Capillary Conductivity from Pressure Plate Outflow Data. *Soil Science Society Proceeding*, 20, 317 - 320.

Hantush, M. S. (1964), Hydraulics of Wells. In *Advances in Hydroscience* (ISSN: 0065-2768, Vol. 1, pp. 281-432). Socorro, New Mexico: New Mexico Institute of Mining and Technology.

526 Khaleel, R., and Relyea, J. F. (1995). Evaluation of van Genuchten-Mualem relationships to
527 estimate unsaturated hydraulic conductivity at low water contents. *Water Resour. Res.,* 31(11),
528 2659-2668.

529 Kunze, R. J., & Kirkham, D. (1962). Simplified Accounting for membrane impedance in
530 Capillary Conductivity Determinations. *Soil Sci. Soc. Am. Proc.*, 26, 421-426.

531 Miller, E., & Elrick, D. (1958). Dynamic determination of capillary conductivity extended for
532 non-negligible membrane impedance. *Soil Sci. Soc. Am. Proc.*, 22, 483–486.

533 Mualem, Y. (1976). A New Model for Predicting the Hydraulic Conductivity of Unsaturated
534 Porous Media. *Water Resources Research,* 12(3), 513-522, DOI:10.1029/WR012i003p00513.

535 Nasta, P., Huynh, S., Hopmans, J. W. (2011). Simplified Multistep Outflow Method to Estimate
536 Unsaturated Hydraulic Function for Coarse Texted Soils. *Soil Sci. Soc. Am. J., 75, 418-425.*

537 Pachepsky, Y., and van Genuchten, M. Th. (2011). Pedotransfer Functions. In Glinski, J.,
538 Horabik, J., Lipiec, J. (Eds.), *Image Analysis in Agrophysics* (pp. 556-561). Springer. DOI:
539 10.1007/978-90-481-3585-1_109.

540 Peters, A., Durner, W., Wessolek, G. (2011). Consistent parameter constraints for soil hydraulic
541 functions. *Advances in Water Resources*, 34, 1352-1365, DOI:10.1016/j.advwatres.2011.07.006.

542 Richards, L. A. (1931). Capillary conduction of liquids through porous media. *Physics*, 1, 318-
543 333.

544 Rijtema, P. E. (1959). Calculation of capillary conductivity from pressure plate outflow data with
545 non-negligible membrane impedance. *Netherlands Journal of Agricultural Science*, 7(3), 209–
546 215.

547 Schaap M. G., and Leij F. J. (2000). Improved prediction of unsaturated hydraulic conductivity

with the Mualem–van Genuchten model. *Soil Sci. Soc. Am. J.*, 64:843–51.

Schelle, H., Iden, S. C., Durner, W. (2011). Combined Transient Method for Determining Soil Hydraulic Properties in a Wide Pressure Head Range. *Soil Sci. Soc. Am. J.*, 75, 1681-1693.

Sivaram, B., & Swamee, P. (1977). A Computational Method for Consolidation Coefficient. *Soils Found. Tokyo*, 17(2), 48–52.

Stanić, F., Jaćimović, N., Ranđelović, A., & Despotović, J. (2017). Laboratory investigation of hydraulic characteristics of fly ash as a fill material from the aspects of pollutant transport. *Water Science and Technology*, 76(4), 976–982.

Stanić, F., Cui. Y.-J., Delage, P., De Laure, E., Versini, P.-A., Schertzer, D., & Tchiguirinskaia, I. (2019). A device for the simultaneous determination of the water retention properties and the hydraulic conductivity function of an unsaturated coarse material; application to a green-roof volcanic substrate. *Geotechnical Testing Journal*, DOI: 10.1520/GTJ20170443.

Stovin, V., Poë, S., De-Ville, S., & Berretta, C. (2015). The influence of substrate and vegetation configuration on green roof hydrological performance. *Ecological Engineering*, 85, 159-172.

Šimunek, J., van Genuchten, M. Th., Šejna, M. (2008). Development and Applications of the HYDRUS and STANMOD Software Packages and Related Codes. *Vadose Zone Journal*, 7, 587-600, DOI:10.2136/vzj2007.0077

Terzaghi, K., & Fröhlich, O. K. (1936). Theorie der Setzung von Tonschichten. Wien, Franz Deuticke: Leipzig.

Valiantzas, J. D. (1989). A Simple Approximate Equation to Calculate Diffusivities from One-Step Outflow Experiments. *Soil Sci. Soc. Am. J.*, 53, 342–349.

569 Valiantzas, J. D. (1990). Analysis of Outflow Experiments Subject to Significant Plate
570 Impedance. *Water Resources Research*, 26(12), 2921–2929.

571 van Dam, J. C., Stricker, J. N. M., Droogers, P. (1994). Inverse Method to Determine Soil
572 Hydraulic Functions from Multistep Outflow Experiments. *Soil Sci. Soc. Am. J.*, 58, 647-652.

573 van Genuchten, M. Th. (1980). A Closed-form Equation for Predicting the Hydraulic
574 Conductivity of Unsaturated Soils. *Soil Sci. Soc. Am. J.,* 44, 892-898.

575 Versini, P.A., Gires, A., Fitton, G., Tchiguirinskaia, I., & Schertzer, D. (2018). Toward an
576 assessment of the hydrological components variability in green infrastructures: Pilot site of the
577 Green Wave (Champs-sur-Marne). *La Houille Blanche*, 4, 34-42

578 Vogel, T., van Genuchten, M. Th., & Cislerova, M. (2001). Effect of the shape of the soil
579 hydraulic functions near saturation on variably-saturated flow predictions. *Advances in Water*
580 *Resources*, 24, 133-144.

581 Wayllace, A. and Lu, N. (2011). A transient Water Release and Imbibitions Method for Rapidly
582 Measuring Wetting and Drying Soil Water Retention and Hydraulic Conductivity Functions.
583 *Geotechnical Testing Journal*, 35(1), 1-15.

584 Yates, S. R., van Genuchten, M. Th., Warrick, A. W., Leij, F. J. (1992). Analysis of measured,
585 predicted, and estimated hydraulic conductivity using the RETC computer program. *Soil Sci.*
586 *Soc. Am. J*. 56, 347–354, DOI:10.2136/ sssaj1992.03615995005600020003x.

587

List of Tables:

List of Figures:

Table 1. Parameters used and permeability values obtained for Gardner's method, our method and Kunze & Kirkham's method for the poorly graded sand and the undisturbed silt clay investigated in Wayllace and Lu (2011)

	Gardner		*This Work*		*Kunze & Kirkham*			
	D $[m^2/s]$	*K [m/s]*	*D* $[m^2/s]$	*K [m/s]*	*a [-]*	t_{RP} *[s]*	λ_1^2 *[-]*	*K [m/s]*
Poorly graded sand	$1x10^{-8}$	$2.01x10^{-9}$	$1.4x10^{-8}$	$2.81x10^{-9}$	0.389	23700	1.3228	$4.58x10^{-9}$
Undisturbed silty clay	$8x10^{-8}$	$2.29x10^{-9}$	$1.4x10^{-7}$	$4.01x10^{-9}$	0.5	2300	1.1596	$6.37x10^{-9}$

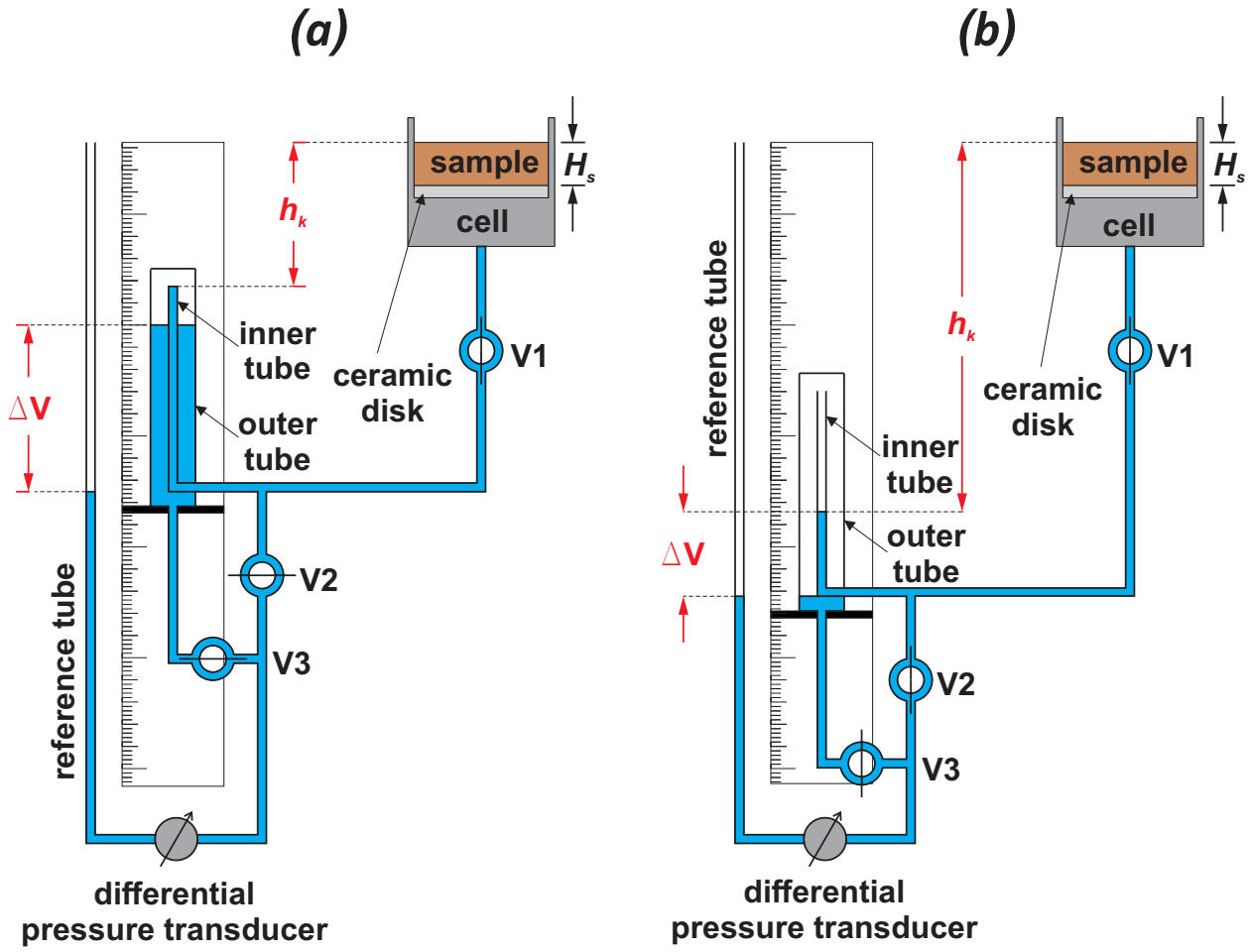

Figure 1. Experimental setup that secures: a) constant imposed suction increment (overflow system); b) non-constant imposed suction increment (After Stanic et al. 2019)

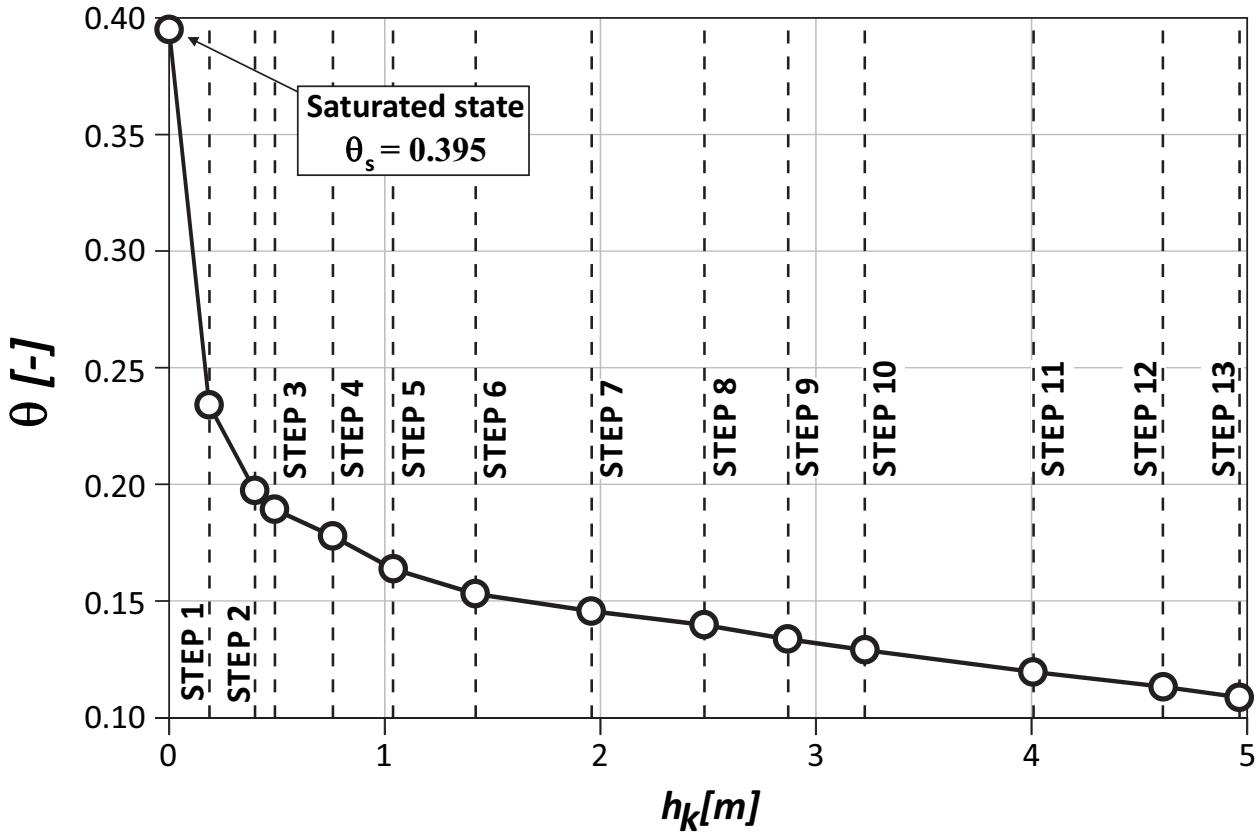

Figure 2. Experimentally determined WRC of the coarse substrate (After Stanic et al., 2019)

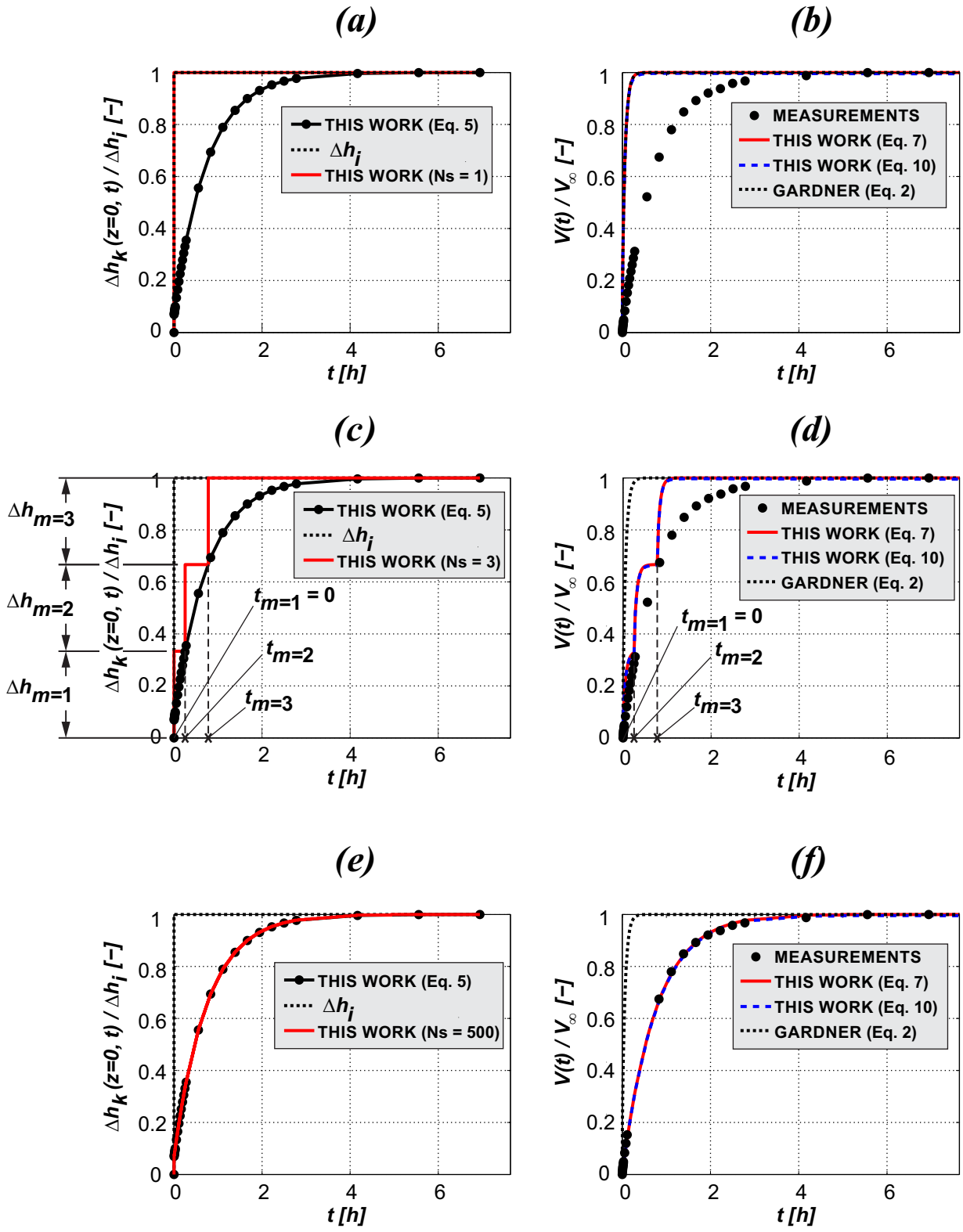

Figure 3. Simulated evolution of drained volumes (b, d, f) using calculated Δh_k (z = 0, t) curve decomposed with Ns = 1(a), 3(c) and 500(e) successive suction increments, respectively. Data from coarse substrate.

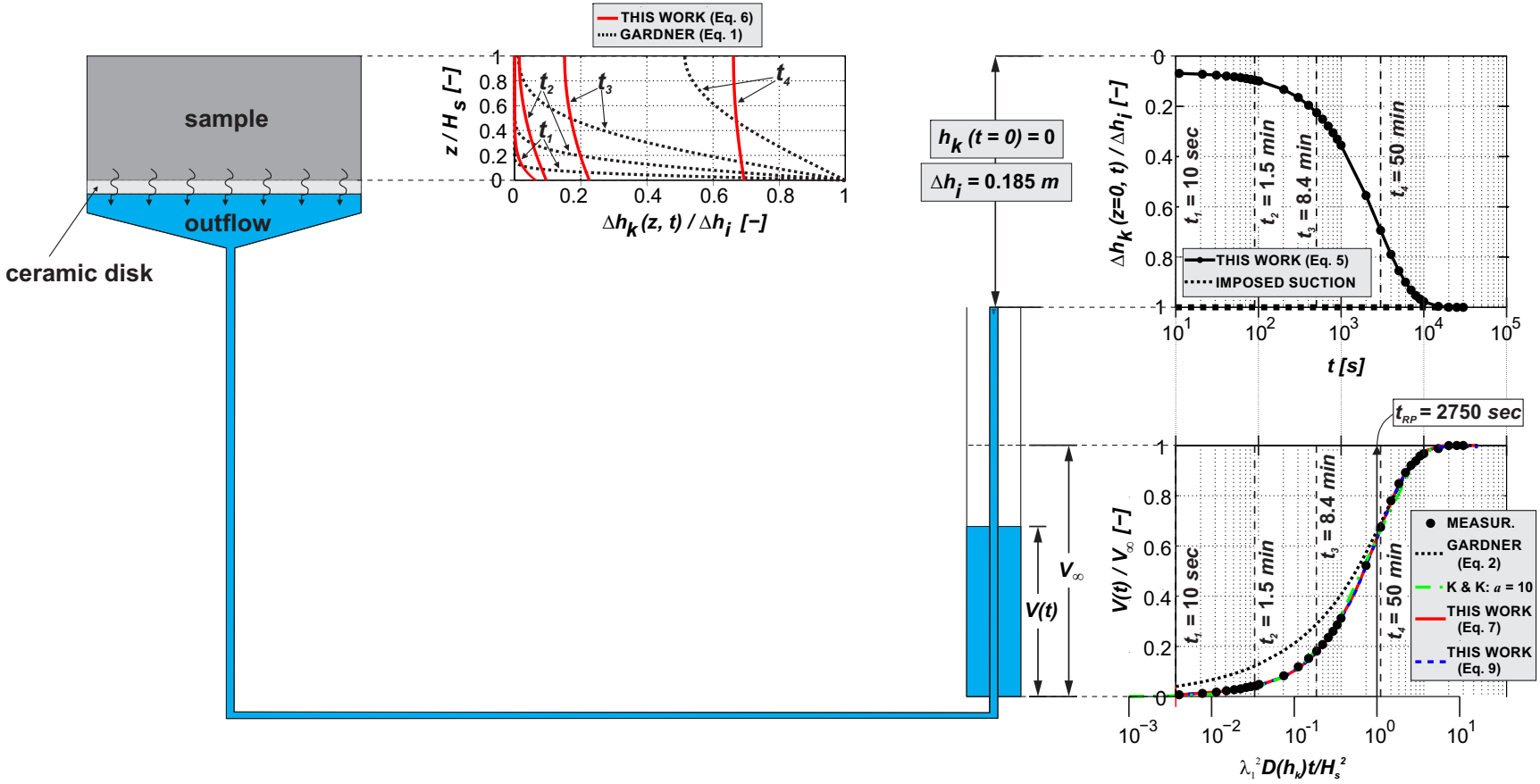

Figure 4. Detailed scheme of implementation of step 1 using the overflow method (constant imposed suction step). Data from coarse substrate.

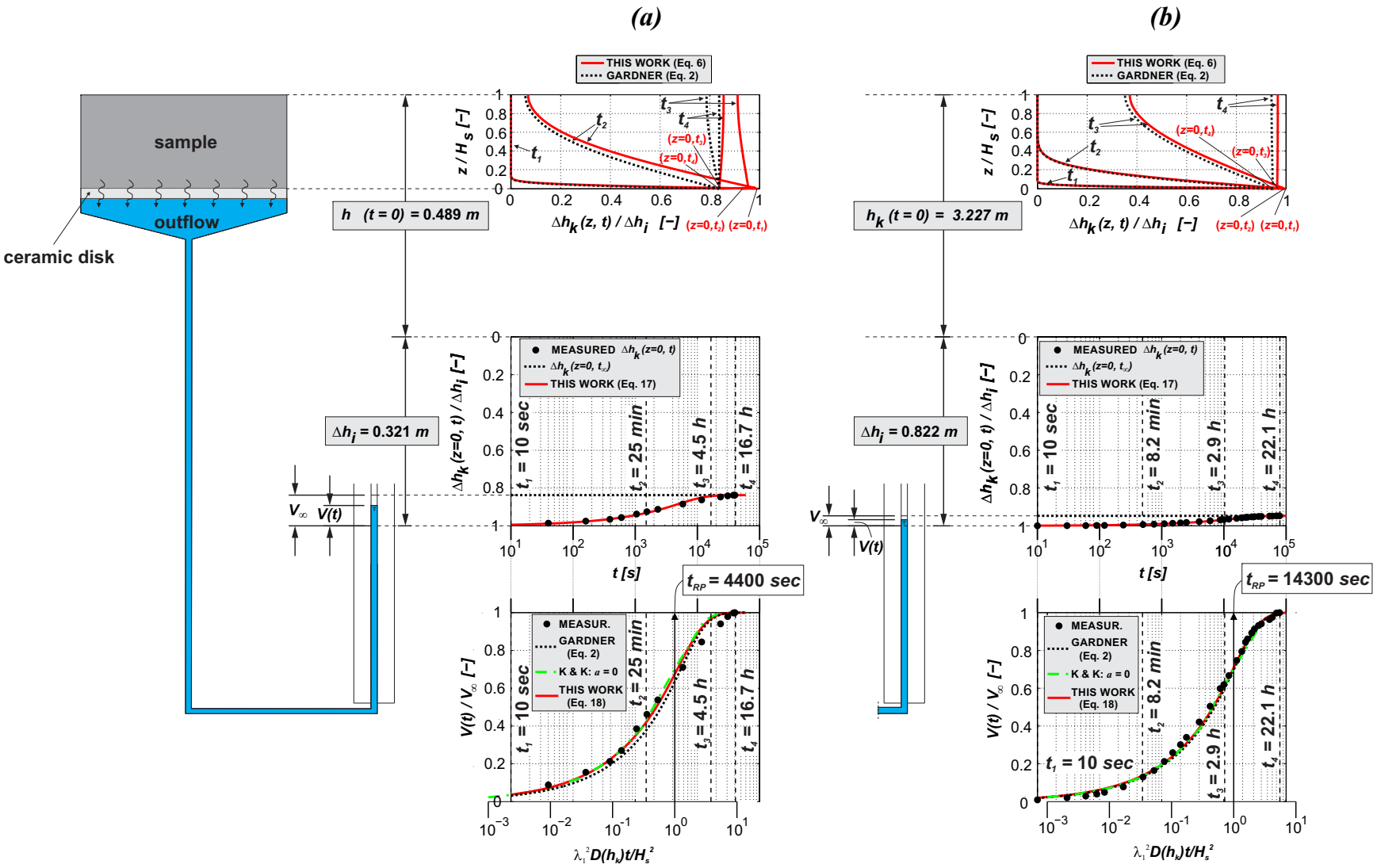

Figure 5. Detailed scheme of implementation of steps 4 (a) and 11 (b) when imposing non-constant suction increment. Data from coarse substrate.

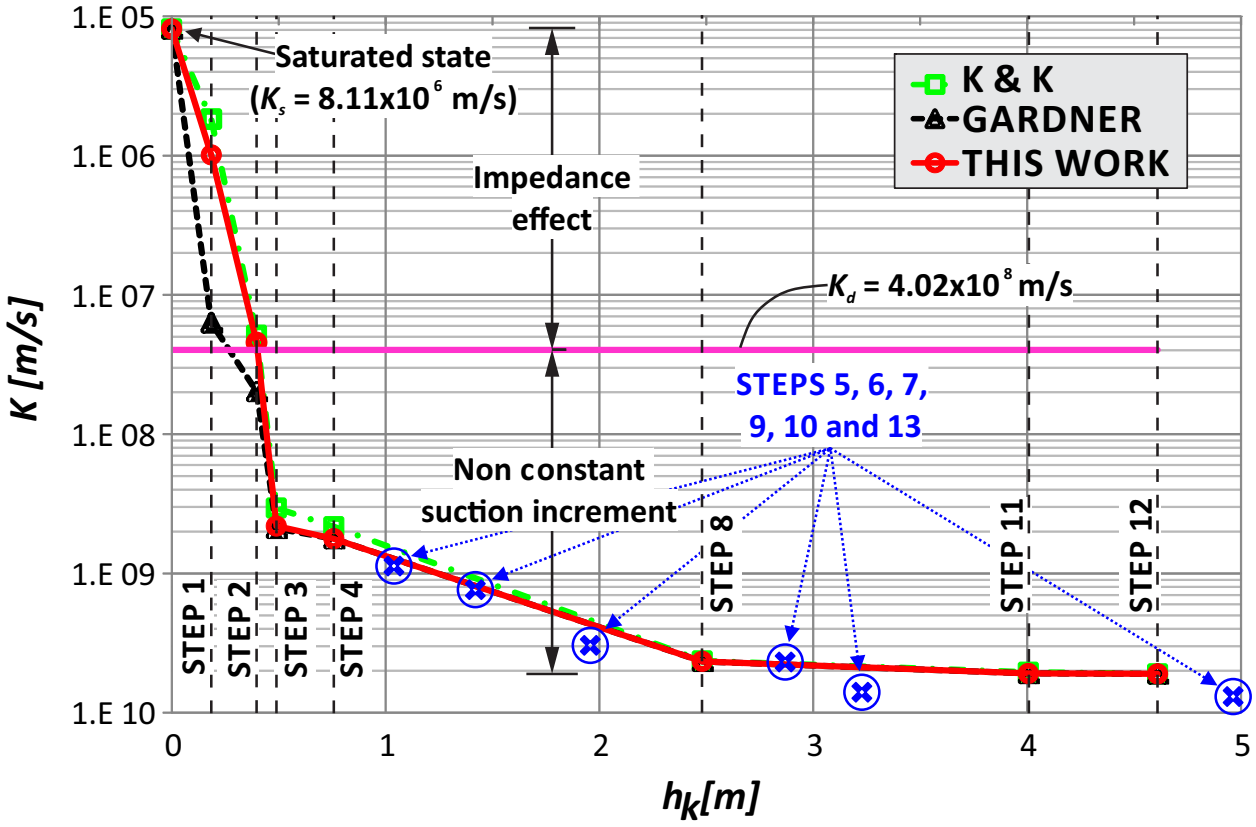

679

680 *Figure 6. Change of hydraulic conductivity of the coarse substrate with respect to increased*
681 *suction obtained using 3 different methods: Kunze & Kirkham's method (squares), Gardner's*
682 *method (triangles) and methods developed in this work (circles). Hydraulic conductivity values*
683 *obtained by analyzing volume change measurements at larger times (Equation 3) are presented*
684 *with blue symbols*

685

686

687

688

689

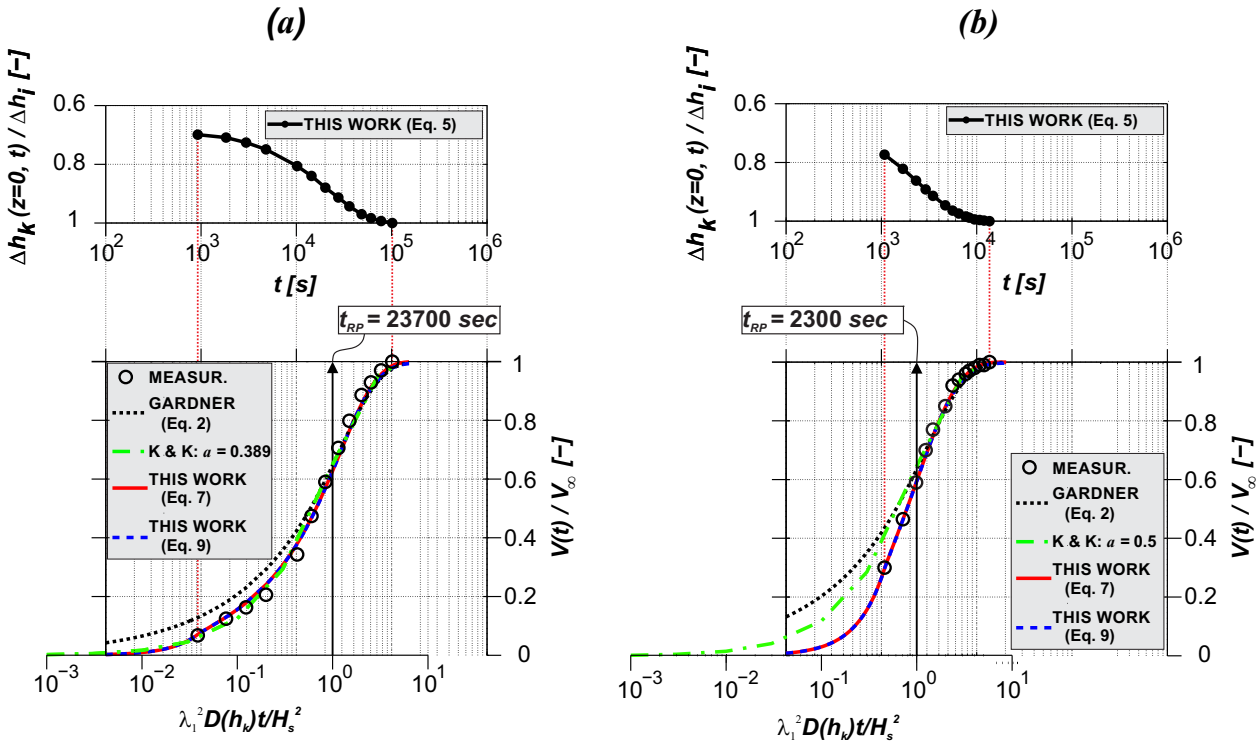

690

691 *Figure 7. (a) Poorly graded sand (data from Wayllace and Lu 2011); top - Suction change at*
692 *specimen bottom, at contact with ceramic disk, bottom – measured outflow (circles) compared*
693 *with calculated values from different methods (indicated on the figure);*
694 *(b) Undisturbed silty clay (data from Wayllace and Lu 2011): same as in (a)*